SANDIA REPORT
SAND2007-7667
Unlimited Release
Printed November 2007

SPECTRAL UNFOLDS OF PITHON FLASH X-RAY SOURCE

E. Frederick Hartman, Thomas A. Zarick and Timothy J. Sheridan
Sandia National Laboratories

John C. Riordan
L-3 Pulse Sciences

Prepared by
Sandia National Laboratories
Albuquerque, New Mexico 87185 and Livermore, California 94550

Sandia is a multiprogram laboratory operated by Sandia Corporation,
a Lockheed Martin Company, for the United States Department of Energy's
National Nuclear Security Administration under Contract DE-AC04-94AL85000.

Issued by Sandia National Laboratories, operated for the United States Department of Energy by Sandia Corporation.

SAND2007-7667
Unlimited Release
Printed November 2007

SPECTRAL UNFOLDS OF PITHON FLASH X-RAY SOURCE

E. Frederick Hartman, Thomas A. Zarick and Timothy J. Sheridan
Sandia National Laboratories

John C. Riordan
L-3 Pulse Sciences

ABSTRACT

Using a differential absorption spectrometer we obtained experimental spectral information for the PITHON Flash X-ray Machine located in San Leandro, California at L-3 Communications. Spectral information we obtained pertained to the 200 keV to 800 keV endpoint operation of PITHON. We also obtained data on the temporal behavior of high energy and low energy spectral content.

ACKNOWLEDGEMENTS

The authors acknowledge the contributions of Niansheng Qi and Sophie Chantrenne of L-3 Pulse Sciences, San Leandro, CA, and compliment the entire PITHON crew for excellent support and contributions on this project. We further acknowledge the contributions in dosimetry support provided by Henry Moeller of SVIC (Boeing Co.) of Ogden, UT. We acknowledge contributions also by S. V. Crowder, SNL. Finally thanks and appreciation go to Diana Wrobel of the Radiation Effects Experimentation Department, SNL for report editing. Radiation Effects Sciences provided funding for this work.

Contents

FIGURES

TABLES

INTRODUCTION

A differential absorption spectrometer technique was used to obtain spectral information for the PITHON Flash X-ray Machine located in San Leandro, California at L-3 Pulse Sciences. Specifically the spectral data we were most interested in obtaining was for PITHON operation using the reflex triode and operating at fairly low end-point energies of about 200 keV and 750 keV.

Our interest in verifying experimentally the calculated or predicted x-ray spectra stemmed from experimental work at PITHON to validate the RAMSES code modules (Ref. 1) for both cable SGEMP (Ref. 2) and box IEMP effects. Cable SGEMP responses are somewhat sensitive to the spectral energy content of the radiation pulse for some types of cable (Ref. 2, 3). This sensitivity is illustrated in Figure 1 for the calculated SGEMP response of a RG-402 coaxial cable. It can be seen that the cable response is positive for photon (or x-ray) energies below 70 keV and negative for photon energies above 70 keV. Clearly, the spectrum for an experiment must be known with reasonable certainty to assure comparisons between codes (performing computational simulations) and experiments (performing physical simulations) are valid.

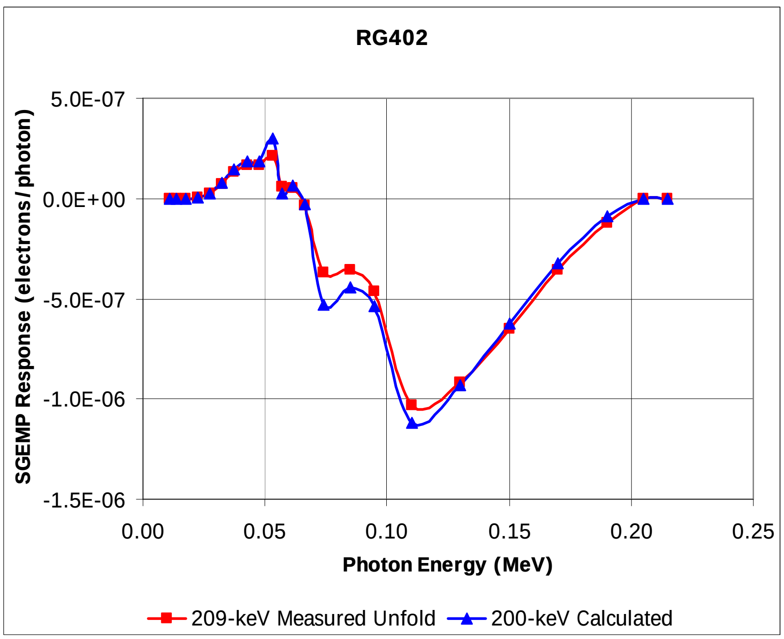

Figure 1 Calculated SGEMP Response of a RG-402 Coaxial Cable

The unfolding technique (Ref. 4) that was used to calculate the x-ray spectral data from our experimental data was developed by L-3 Pulse Sciences (formerly Titan Pulse Sciences Division). The data input to the unfold code consists of measured dose behind a set of prescribed x-ray filter materials for the specific end-point energies of interest. The dose measurements were made using thermo-luminescent dosimeters (TLDs) of calcium fluoride (CaF_2) or lithium fluoride (LiF) type. We also performed some experiments that included time-resolved information by using PIN diodes behind the various filter material stacks and recording the PIN diode signals in time.

This report provides some information on the unfold technique. A complete description of the unfold technique is provided in reference 4. The experiments that were performed to obtain data for determining the x-ray spectra are described and documented, and finally the results of unfolded data are compared to computer model predictions of the x-ray spectra (Ref. 5).

1 THE UNFOLD METHOD

One standard method for measuring x-ray spectra is the differential absorption spectrometer (DAS), which uses a number of identical detectors with different x-ray filters.

The x-ray spectrum must be unfolded from the DAS data, typically using an iterative perturbation method. In this method one assumes an initial (trial) spectrum and then uses known response functions for the filtered detectors to calculate the individual detector doses. Next one defines a set of basis functions for the filtered detectors to span the entire spectral range; each basis function multiplies the spectrum over a limited energy range, e. g., rectangular step functions. Then one iteratively adjusts the spectrum by varying the basis multipliers to minimize the error between the measured and calculated doses.

The conventional unfold solutions typically suffer from several shortcomings. First, the unfolded spectrum depends strongly on the choice of the initial trial spectrum, i.e., it is not unique. Second, the spectrum contains peaks that are physically impossible. Third, the endpoint energy must be specified a priori, or by the ratio of several DAS signals. The parametric approach used in this report for the most part overcomes these problems.

Riordan and Qi have developed a new Low-Energy Differential Absorption Spectrometer (LEDAS) technique for use on the PITHON High-Fidelity (Warm) Reflex Triode (Ref. 6). In the parametric unfold approach, the spectrum is represented as a function of a limited number of parameters that are directly related to physical processes involved in relativistic electron Bremsstrahlung sources. In particular, we write the spectral intensity (energy/area/MeV) as a product of a scale factor C and three functions for Bremsstrahlung, x-ray absorption, and K-shell features.

The unfold procedure also uses an iterative perturbation approach to minimize the difference between measured and calculated doses in the filtered detectors. To begin the process, one specifies an initial (non-critical) guess for the 8 free parameters and then uses the DAS response functions R(E) (which are determined by the DAS filters and detectors) to calculate the doses to each of N detectors:

$$D_i^{calc} = \int dE \ \mathrm{S(E)\ R_i\ (E),\ I = 1,2\ \ldots N}$$

Then one calculates a root-mean-square (rms) relative error:

$$E = \sqrt{\frac{\sum_{i=1}^{N} 4W_i \left(\frac{D_i^{calc} - D_i^{meas}}{D_i^{calc} + D_i^{meas}}\right)}{\sum_{n=1}^{N} W_i}}$$

W_i are the weighting factors that can be used to eliminate dubious individual measurements. Use of a relative (rather than absolute) error is necessary to ensure a good match to the dose in the most heavily filtered detectors, which have the smallest measured doses. These detectors are critical for determining the high-energy tail of the spectrum.

Next one iterates on the free parameters to minimize rms error. Riordan and Qi chose the computationally robust Downhill Simplex Method to perform the minimization. This method requires an initial guess (which can be a crude guess) and an initial perturbation step (which we typically set to half the initial step) for each parameter, and then we automatically iterate on the parameters and step sizes. The method requires only function calls (not derivatives) and is especially well suited for highly non-linear functions. The minimization terminates when rms error cannot be reduced beyond a factor (typically 10^{-4}) specified by the user. The Downhill Simplex Method (Ref. 7) is computationally inefficient, but converges to a solution.

By iterating upon the parameters we are effectively replacing the local perturbations of the basis functions with global perturbations that are physically reasonable. This improves the likelihood of finding a global rather than a local minimum for the error. This gives a unique solution that is independent of the trial spectrum and contains no non-physical features. The parametric unfold procedure has been implemented in a code DAS Unfold, which is written in Interactive Data Language (IDL) and runs on either Windows or Mac OS-X platforms.

2 THE LOW ENERGY DIFFERENTIAL ABSORPTION SPECTROMETER

In the parametric unfold technique we express the spectrum as a function of parameters such as endpoint energy, low energy cutoff, K-line fraction, K-edge absorption notch, and a scalar factor. Physical models for the energy dependence of thin-target Bremsstrahlung and x-ray absorption cross-section determine the spectral shape. Using the parameter spectral representation, one calculates the expected DAS signals and compares them to measured DAS signals. Then the root-mean-square error is minimized by using the downhill simplex method. The method requires as input an initial value and an initial perturbation step for each of the parameters. This technique was evaluated and validated by J. Riordan and S. Chantrenne of Titan Pulsed Sciences in cooperation with V. Harper-Slaboszewicz of Sandia National Laboratories.

Riordan, Chantrenne, and Harper-Slaboszewicz evaluated the techniques using a 9-channel temporally resolved spectrometer (TDAS) supplied by Sandia National Laboratories. They performed unfolds of both "theoretical" TDAS data from a TIGER-calculated spectrum with an endpoint energy of 309 keV and measured data from an experiment on PITHON for a measured peak diode voltage of 328 keV. Despite a wide variation in initial parameters, they found that the unfold procedure converged to the same solution. The rms signal error was typically about 1% and the unfolded spectrum was within about 3% of the true spectrum. The Sandia TDAS response functions for Harper-Slaboszewicz's temporally-resolved spectrometer are given in Figure 2. Also included in the figure are the materials and corresponding thicknesses used in the TDAS.

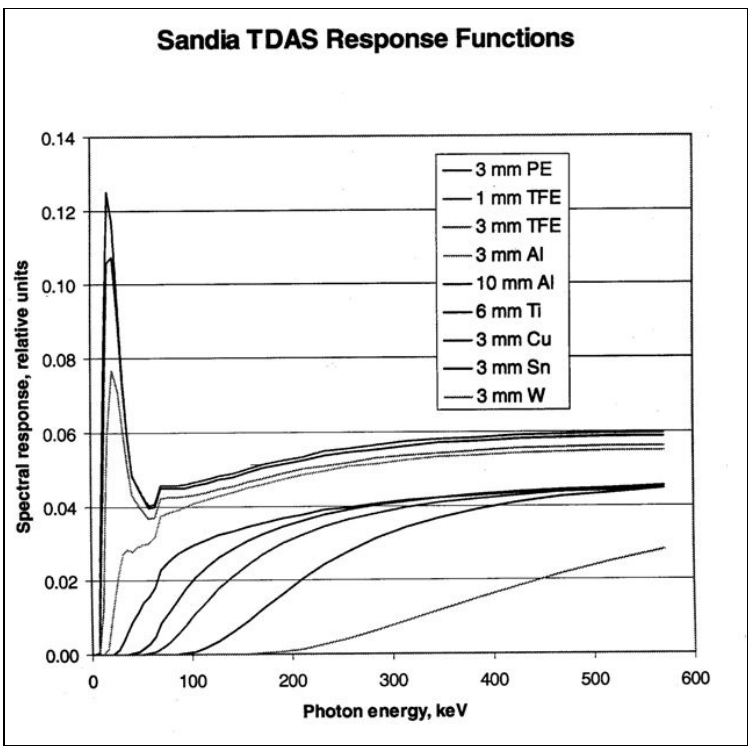

Figure 2 Sandia TDAS Response Functions

Figure 3 shows the relative insensitivity of the spectral convergence as the doses for each TDAS channel are varied one at a time theoretically by 10%.

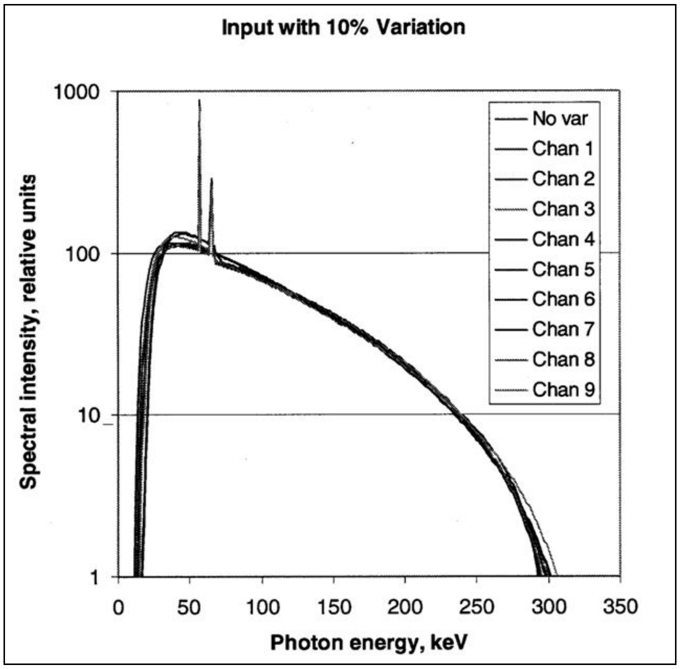

Figure 3 Relative Insensitivity of the Spectral Convergence

Another comparison in which the initial input parameter of endpoint energy was varied from 200 to 400 KeV is shown in Figure 4. In this case an unfold procedure was performed with experimental TDAS data for each of three endpoint energies of 200, 300, and 400 keV.

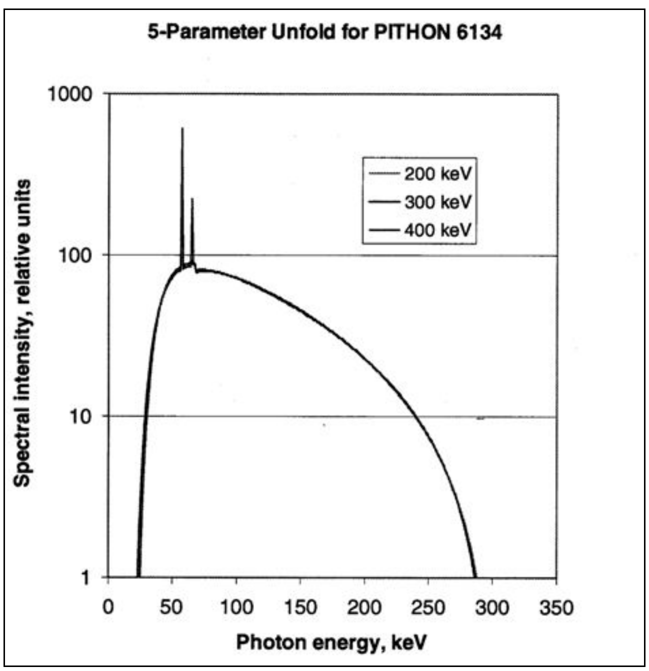

Figure 4 5-Parameter Unfold

We, the authors, and Titan Pulse Sciences (now L-3 Pulse Sciences) each designed new DAS tailored to the PITHON machine endpoint energies of 200-250 KeV, and we designed another DAS tailored to a PITHON endpoint energy of about 750 KeV. These designs, through material selection for the individual channels, also improved the resolution near the K-edge over the previous design. Our DAS both for the 200 KeV and 750 KeV spectra had the capability of 16 channels. For the 200-250 endpoint DAS, we used 10 unique filter materials with 6 of the materials duplicated for consistency checks. For the 750-KeV endpoint we used 13 channels with 3 duplicate channels. The DAS were designed to accommodate up to 6 TLDs per channel and could be used to acquire temporal responses using PIN diodes behind each of the individual filters. Descriptions of these DAS designs and the experimental results of the spectral unfolds are given in the next sections of this report.

3 EXPERIMENTAL RESULTS AT 200 KEV ENDPOINT

A 16-channel DAS was used to record data for spectral unfolds at PITHON endpoint energies near 200 keV. It was determined that 10 channels of unique filtered data were sufficient to characterize the spectrum, so 6 channels were duplicates that recorded dose data for 6 identical filter pairs. For each filter channel we typically used 3 LiF and 3 CaF_2 TLDs. We calibrated the TLDs to a unique X-ray spectrum very similar to the spectra we expected PITHON to produce for an endpoint of about 200 keV behind each filter. The calibrations were performed using a continuous x-ray source (Ref. 8). The TLD data were unfolded using the techniques previously described to produce a measured spectrum.

Our 16-channel DAS filter stack including each material and thickness is described in Table 1.

Table 1 16-channel DAS Filter Stack

A PNS09 "None" 1	B PNS07 1 mm Al 2	C PNS06 0.3 mm Cu 4	D PNS202 3 mm Sn 7
E PNS206 0.625 mm Ho 9	*F* *PNS203* *0.225 mm Ta* *10*	*G* *PNS208* *1 mm W,* *1.5 mm Sn* *8*	H PNS205 3 mm Cu 6
I *PNS207* *3 mm Sn* *7*	*J* *PNS02* *0.3 mm Cu* *4*	*K* *PNS209* *0.625 mm Ho* *9*	L PNS201 0.225 mm Ta 10
M PNS204 1 mm W, 1.5 mm Sn 8	N PNS04 1 mm Cu 5	O PNS05 4 mm Al 3	*P* *PNS08* *"None"* *1*

250 keV Filter stack - Italic & Underlined are backups

The stack as pictured in Table 1 is basically a pictorial representation of the relative locations of the various filters assuming radiation from PITHON was incident on the backside of the fixture shown at the top of the photograph below. A photograph of the DAS with filters installed is shown in Figure 5 at the top of the photograph.

Figure 5 DAS with Filters Installed

The filters were mounted within an aluminum holding fixture shown lower right in Figure 5. Also shown in the same figure at lower left is the holding plate for the six TLDs per channel and a center opening through which PIN diodes were mounted to record time-resolved dose rate information for some of the experiments. A K-metal (Tungsten/Cu) edge filter was used on some experiments to provide more isolation filtering between channels and to reduce side scattering from the aluminum holding fixture. In addition, when the time-resolved information was not recorded, we used a holding plate that moved the 6 TLDs closer to the center of the filters to further reduce side scatter effects.

The choice of the number of TLDs at each filter stack location was based on the minimization of error in the dose recorded at each of 16 stack locations and the tradeoff with the costs and complexity of making the fixture bigger and handling and paying for and reading large numbers of TLDs.   We found 3 to 6 TLDs at each location to be sufficient to obtain adequate statistics, as discussed below. To enhance beam uniformity, we performed most experiments at about 1 meter from the face of the PITHON machine. We threw out spectral or dose non-uniformities greater that 10% from being considered in the unfold data sets (the whole data set was not used if dose variations were greater than expected).

We assumed that with good handling techniques, a calibrated electronic TLD reader, and the same person handling all TLDs throughout the various tests that variation would be minimized. We also assumed that TLD standard variation ("sigma") would fall between 6 and 10% for single-batch TLDs. We did not know for sure that the TLDs would have a normal probability distribution, but assumed that this would be the case for calculating the likelihood that 3 or 6 TLDs would differ from the average of all the TLDs on a particular shot (3 x 16 = 48 or 6 x 16 = 96). The solution approach to calculating statistical variation probabilities was to record how many times, out of 100,000 simulation trials of the experiment, that either the maximum or minimum was more than P% different than the overall mean[1].

With 3 TLDs per channel the likelihood was about 4% that any one measurement (average of 3 TLDs) would differ by more than 10% from the overall mean of 48 TLDs for an assumed sigma of 6%. If the sigma was assumed to be greater at 10%, then any one measurement (3 TLD average) would differ by more than 10% almost 70% of the time. The three TLD average would be within 20% of the overall mean in 95% of the locations, however, even for a sigma of 10%.

Using 6 TLDs per location as we did in most cases (though sometimes 3 CaF_2 and 3 LiF) resulted in much better statistics. Assuming a TLD distribution of 6%, the likelihood of a 6-TLD average differing from the mean of the 96 total TLDs is below 1%. For a larger TLD sigma of 10%, there is a 17% likelihood that any one measurement would differ from the mean of the others by more than 10%. Figures 6 through 9 give the distribution histograms for each of the cases previously discussed.

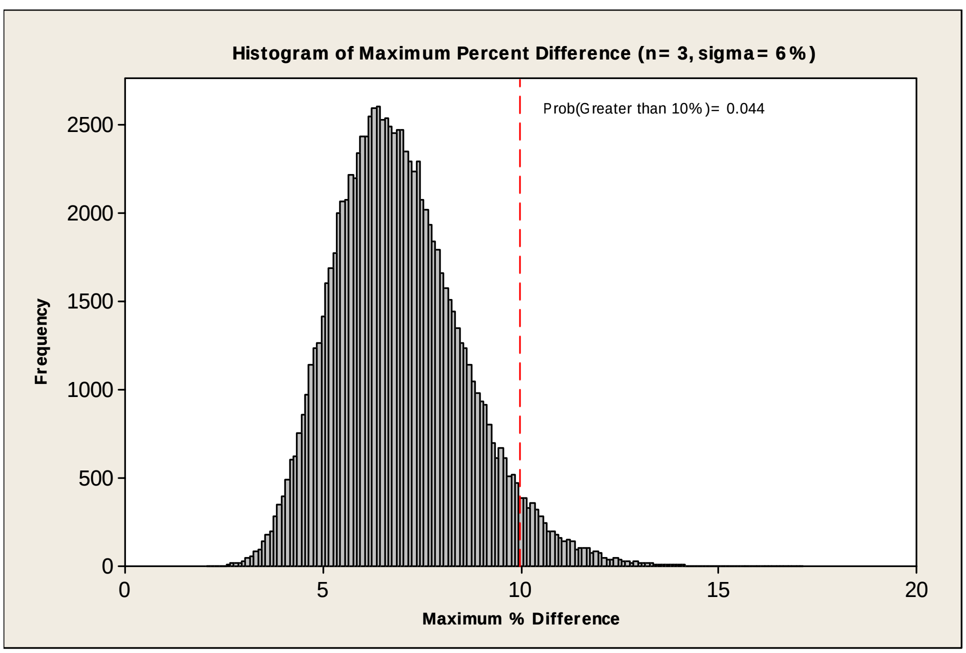

Figure 6 Maximum Percent Differences when n = 3, = 6%

[1] Private communication S.V. Crowder, SNL

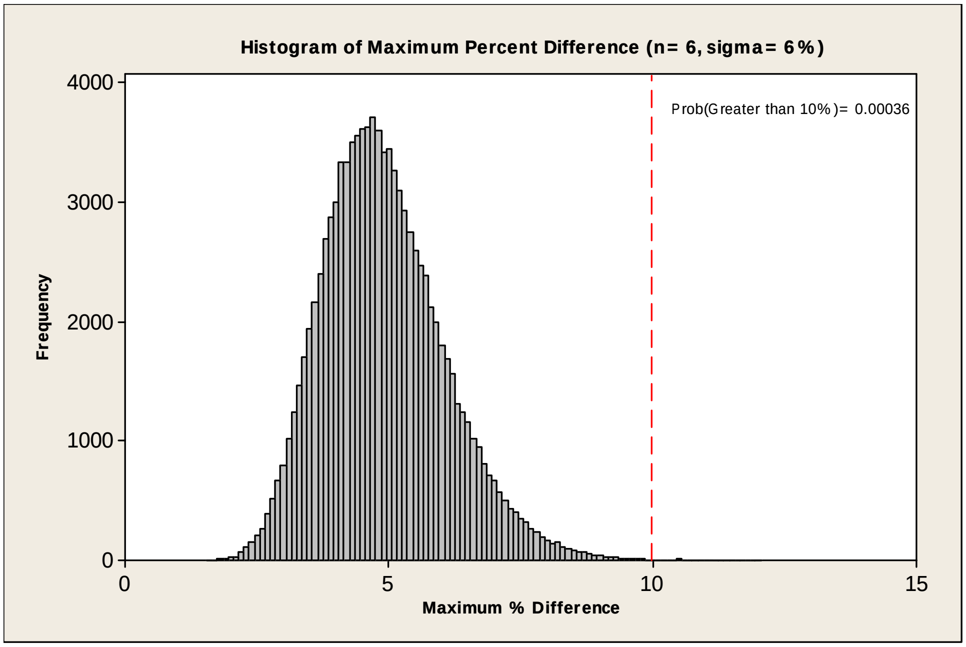

Figure 7 Maximum Percent Differences when n = 6,   = 6%

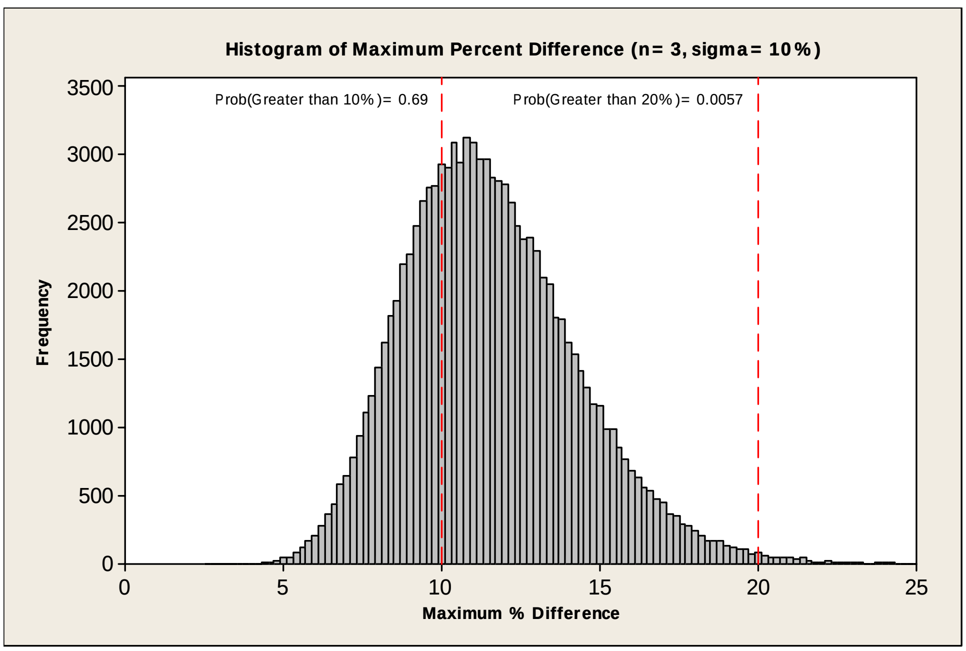

Figure 8 Maximum Percent Differences when n = 3,   = 10%

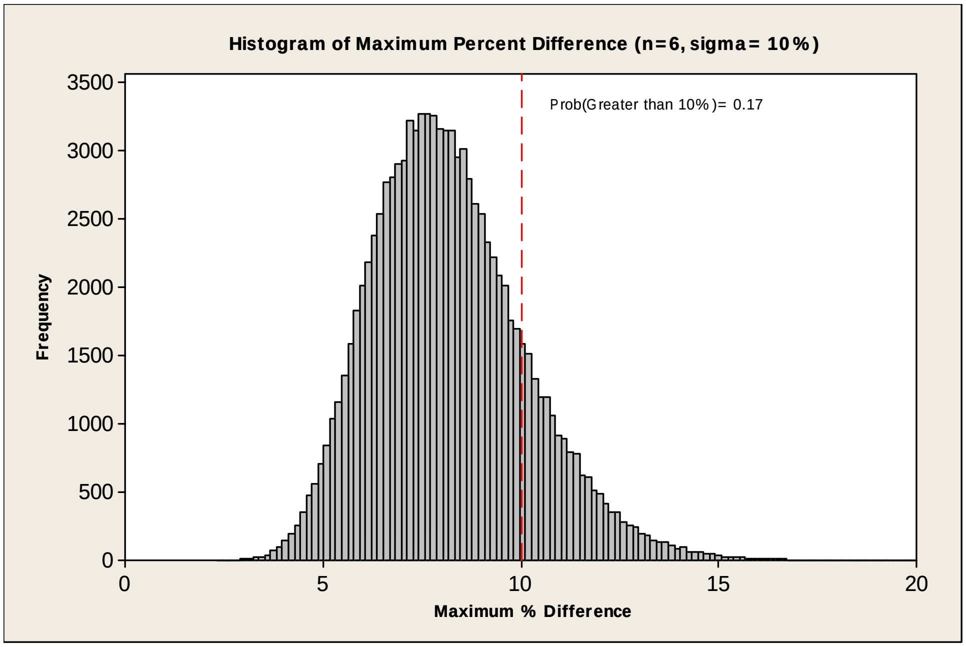

Figure 9 Maximum Percent Differences when n = 6,   = 10%

Response functions were calculated for the filter stack for the DAS design tailored to an endpoint energy of 200 keV on PITHON. Figure 10 shows these response functions for each of the 10 separate filter stacks that are detailed in Table 1.

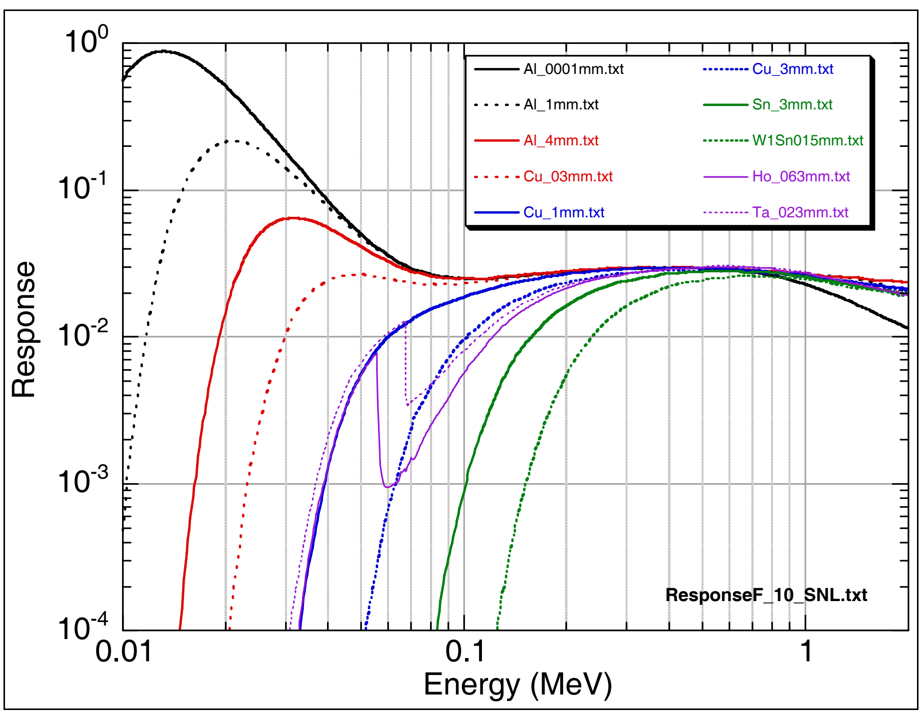

Figure 10 Response Functions for 200 keV - Endpoint DAS

Using these response functions and the methods described previously, the experimental data was unfolded to compare to calculated spectra. Figure 11 shows a comparison of a 200-keV calculated PITHON spectra to a 209-keV unfold of measured data.

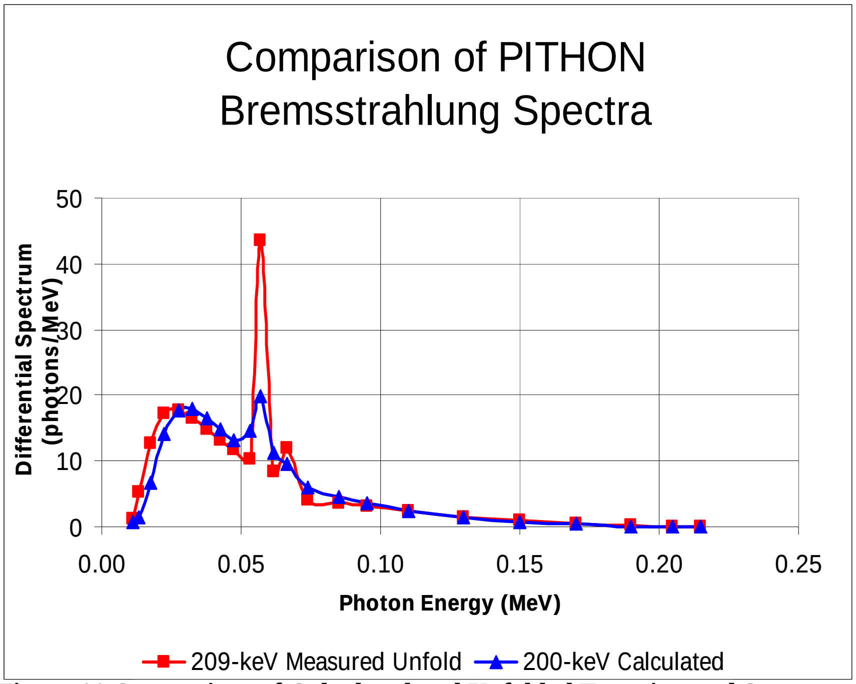

Figure 11 Comparison of Calculated and Unfolded Experimental Spectra

As can be seen the results are in reasonable agreement. For validation, the code validation calculations can be performed separately with both a calculated spectrum and an experimental spectrum to evaluate how sensitive the calculations are to the slight variations in spectra for the same or nearly the same endpoint energies.

4 EXPERIMENTAL RESULTS AT 750 KEV ENDPOINT

For some validation experiments we performed experiments at higher endpoint energy on the PITHON machine. Therefore we designed a separate DAS so our measurements would provide better resolution to the higher energy spectral content. It was found that a DAS with 13 separate filter stacks, rather than 10 filter stacks that were sufficient for the lower energy spectra, provided better resolution for higher energy spectra at about 750-KeV endpoint.

The various filter materials and the thickness of each material in the stacks is given in Table 2.

Table 2 750 KeV Spectrometer PIN Assignment

A P09F1 (PNS09) "None" 1 LiF2 & CaF2 TLD's 1-6	B P07F2 (PNS07) 1 mm Al 2 LiF2 & CaF2 TLD's 7-12	C P06F4 (PNS06) 0.3 mm Cu 4 LiF2 & CaF2 TLD's 13-18	D P202F7 (PNS202) 3 mm Sn 7 LiF2 & CaF2 TLD's 19-24
E P206F9 (PNS206) 0.625 mm Ho 9 LiF2 & CaF2 TLD's 25-30	F P207F13 (PNS207) 10 mm W 13 LiF2 & CaF2 TLD's 31-36	G P209F11 (PNS209) 3 mm W, 1 mm Sn 11 LiF2 & CaF2 TLD's 37-42	H P205F6 (PNS205) 3 mm Cu 6 LiF2 & CaF2 TLD's 43-48
I P203F12 (PNS203) 6.2 mm W 12 LiF2 & CaF2 TLD's 49-54	J P02F5 (PNS02) 1.0 mm Cu 5 LiF2 & CaF2 TLD's 55-60	K P08F1 (PNS08) "None" 1 LiF2 & CaF2 TLD's 61-66	L P201F10 (PNS201) 0.225 mm Ta 10 LiF2 & CaF2 TLD's 67-72
M P204F8 (PNS204) 1 mm W, 1.5 mm Sn 8 LiF2 & CaF2 TLD's 73-78	N P04F5 (PNS04) 1 mm Cu 5 LiF2 & CaF2 TLD's 79-84	O P05F3 (PNS05) 4 mm Al 3 LiF2 & CaF2 TLD's 85-90	P P208F13 (PNS208) 10 mm W 13 LiF2 & CaF2 TLD's 91-96

(RADS Into Page +)

Using these filter materials, response functions were calculated for each of the 13 separate filters. These response functions are given in Figure 12.

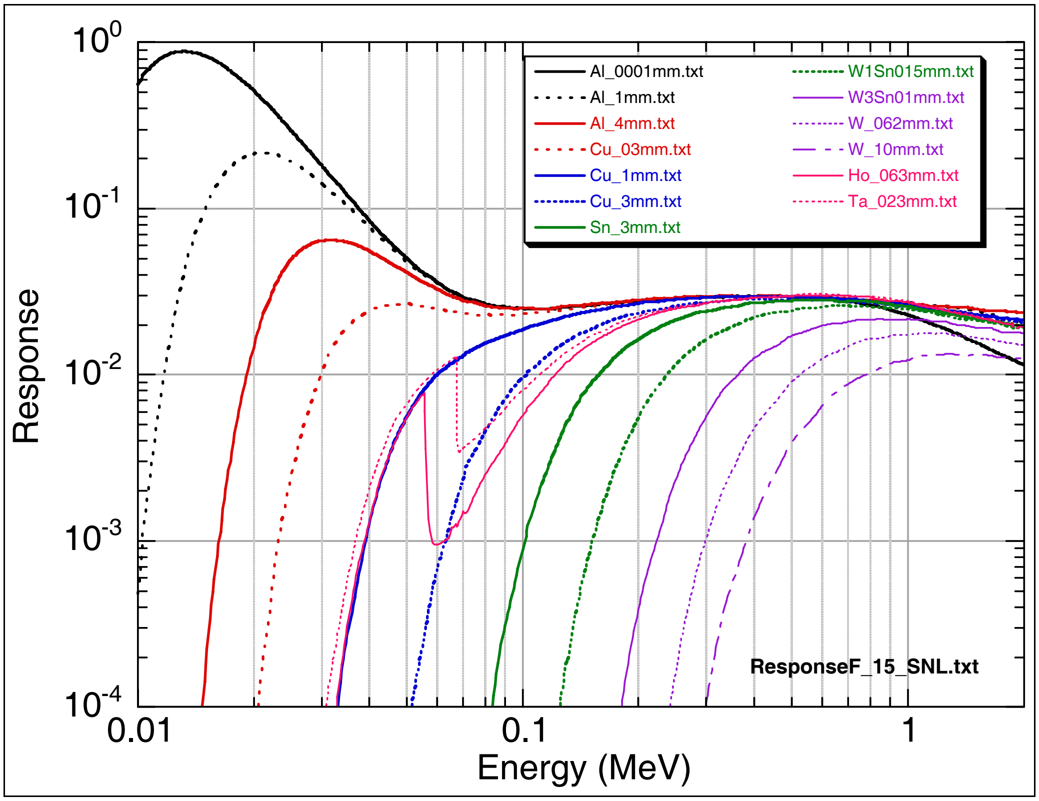

Figure 12 Response Functions for 750-kev Endpoint DAS

Figure 13 provides a comparison of the unfolded spectrum for PITHON shot number 7233 with and endpoint energy of 796 keV with a "standard" 750 keV spectrum calculated using TIGERP.

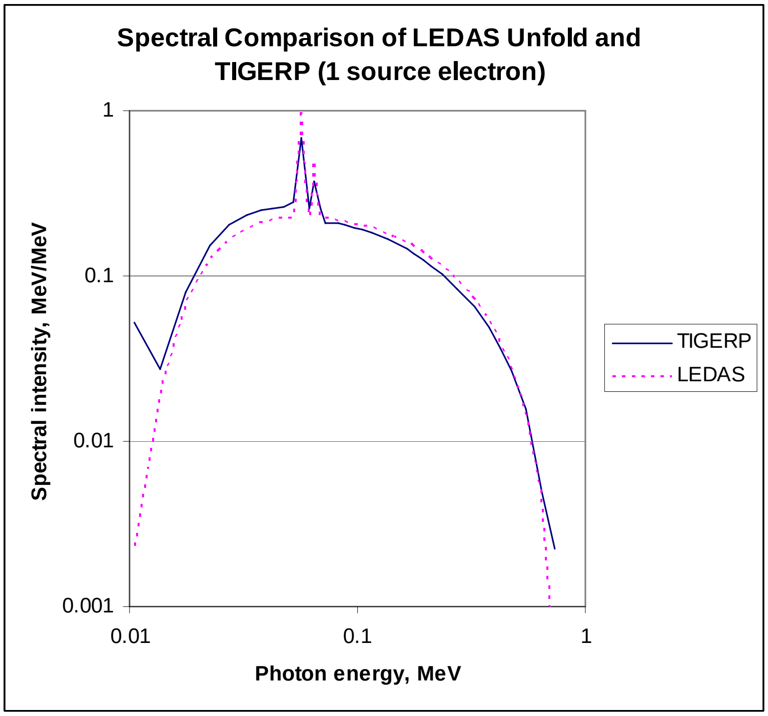

Figure 13 Spectral Comparison of LEDAS Unfold and TigerP Calculations

The L-shell lines near 10 keV are included in the TIGERP calculation, but were not included in the unfolding of the experimental data. For the unfold we left out two TLD channels that were heavily filtered and seemingly outside reality to enhance convergence to a solution.

5 TIME-DEPENDENT SPECTROMETER RESULTS

We had the ability to record PIN diode time-resolved data behind each filter stack in our LEDAS design. The PINs were individually calibrated and PINs with different volumes and sensitivities were used because the dose rates behind the filter stacks varied at least 3 orders of magnitude because of heavy filtering at some positions. We used the PIN data to look at the time dependence of the various channels. We specifically wanted to make sure that duplicate filters of the same material stack had comparable temporal responses. We also wanted to determine if heavily-filtered PINs would respond differently from lightly-filtered PINs. This information would provide evidence whether higher energy x-rays emitted from the PITHON front face had a different temporal signature than lower energy x-rays.

Data from PIN diodes on the same PITHON shot with nominal 200-keV endpoint energy (behind separate but identical filtering) had the same temporal behavior for all cases examined. A typical result for PITHON shot number 7101 and two identical filters of 1.0 mm of Tungsten and 1.5 mm of Tin is shown in Figure 14.

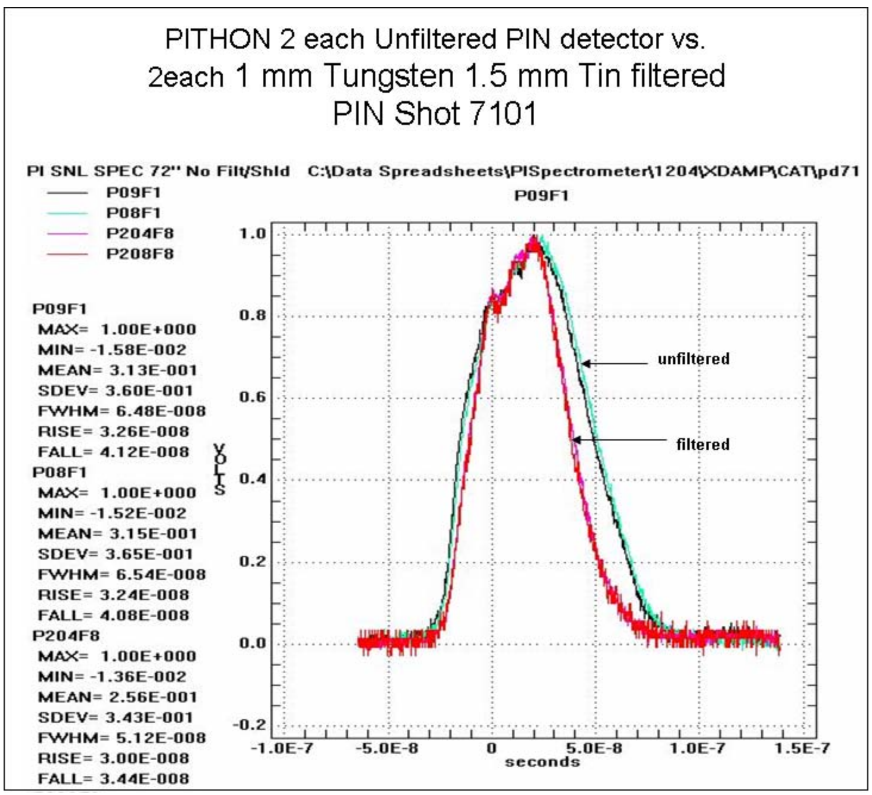

Figure 14 Unfiltered Pair and Filtered Pair Comparisons

The two PIN diode traces essentially are identical. Also shown in the same figure are two identical traces for unfiltered PIN diode responses. These traces have a greater FWHM than the two filtered traces as will be discussed later. The fact that both pairs of traces with identical filtering behave the same is another indication of beam uniformity.

Another comparison of spatial uniformity is provided by examining the uniformity of all 16 PIN diodes in the TDAS under identical thin copper filtering on the same PITHON shot. Figure 15 provides this data for a 200-KeV endpoint operation on PITHON shot number 7093.

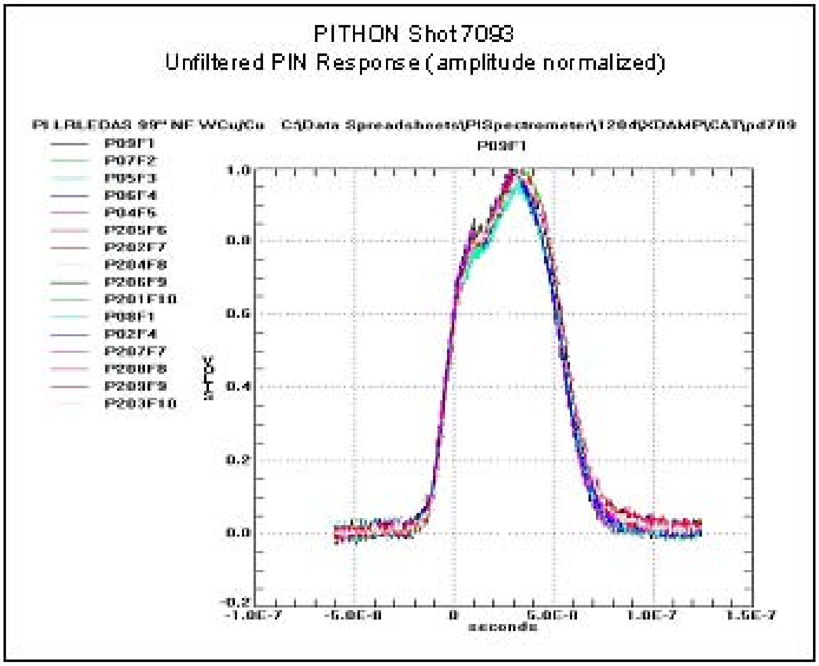

Figure 15 Plots Showing Agreement of All 16 PIN Diodes when Identically Filtered

As can be seen in Figure 15 when all PIN diodes have identical filtering, the temporal agreement of all PINs is excellent.

Now we were especially interested in the time history of higher energy x-rays produced by PITHON operation compared to lower energy x-rays. In general, we found experimentally that the higher energy x-rays had a shorter pulse width (FWHM) than the lower energy x-rays. We are able to make that statement by examining heavily filtered channels on our TDAS (lower energy x-rays are absent) in comparison to lightly filtered TDAS channels which do not remove the lower energy x-rays. Figure 16 shows such a comparison for PITHON shot number 7096 (201-KeV endpoint energy), and Figure 17 provides a similar comparison for PITHON shot number 7148 (777-KeV endpoint energy).

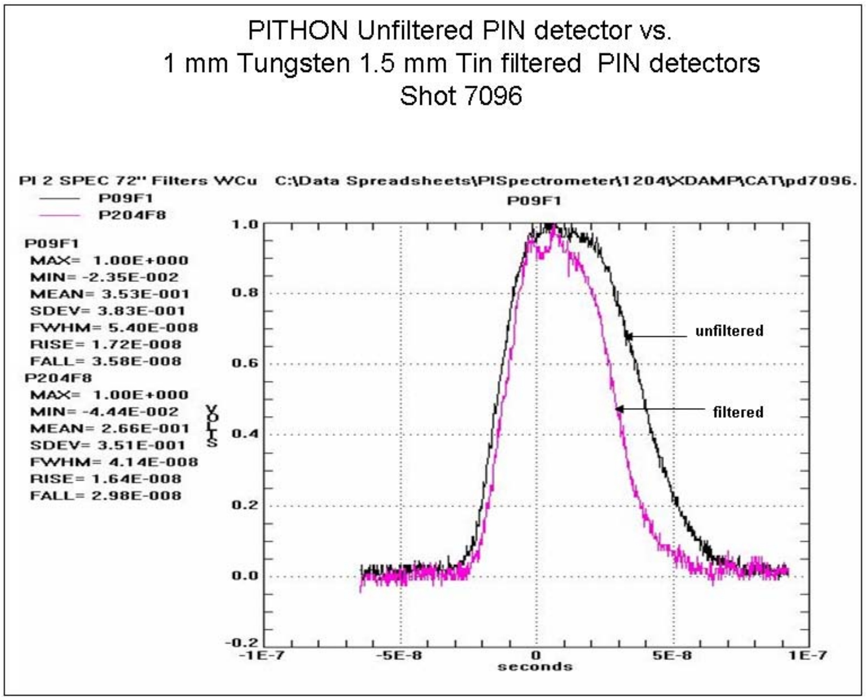

Figure 16 Unfiltered and Filtered PIN Diode Response

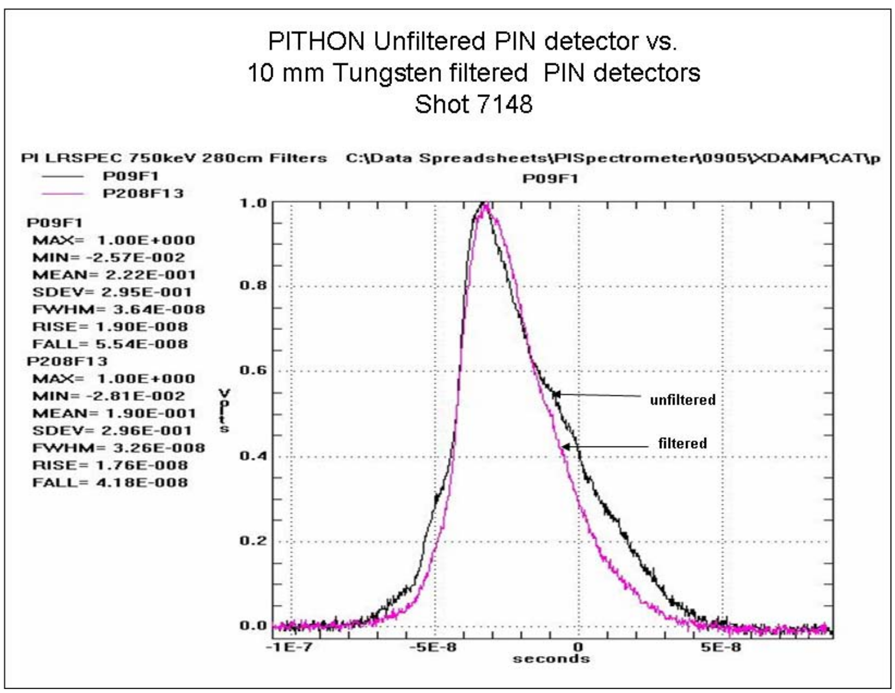

Figure 17 Comparison of Filtered and Unfiltered PIN Diode Response

The difference in pulse width for each filter stack for the lower energy PITHON operation is tabulated in Table 3 for shot numbers 7096 - 7098.

end point (power-wt.)	7096 201keV		7097 194keV		7098 166keV			7148 777keV	
Filters	Rad(CaF2)	FWHM	Rad(CaF2)	FWHM	Rad(CaF2)	FWHM	Filters	Rad(CaF2)	FWHM
Bare	40.07	5.40E-08	2.34E+02	5.32E-08	1.26E+02	3.12E-08	Bare	50.36	3.70E-08
Bare	38.55	5.40E-08	2.11E+02	5.34E-08	1.22E+02	3.32E-08	Bare	49.39	Saturated
1 mm Al	32.24	5.30E-08	1.82E+02	5.28E-08	9.94E+01	3.28E-08	1mm Al	42.97	3.82E-08
4 mm Al	22.13	5.32E-08	1.02E+02	5.24E-08	6.38E+01	3.12E-08	4mm Al	27.20	3.72E-08
0.3 mm Cu	11.73	5.16E-08	6.77E+01	5.08E-08	3.83E+01	3.04E-08	.3mm Cu	18.61	3.48E-08
0.3 mm Cu	14.37	5.16E-08	6.81E+01	5.14E-08	3.82E+01	2.90E-08	1mm Cu	11.10	3.42E-08
1 mm Cu	8.70	4.92E-08	2.46E+01	4.76E-08	1.72E+01	2.74E-08	1mm Cu	10.01	3.78E-08
0.225 mm Ta	3.06	5.04E-08	1.92E+01	5.64E-08	1.05E+01	3.80E-08	.225mm Ta	8.38	Saturated
0.225 mm Ta	3.08	5.08E-08	1.76E+01	5.70E-08	1.12E+01	3.70E-08	.625mm Ho	6.71	3.86E-08
0.625 mm Ho	1.89	4.94E-08	1.09E+01	5.48E-08	7.21E+00	3.30E-08	3mm Cu	5.94	3.84E-08
0.625 mm Ho	1.90	4.92E-08	1.12E+01	5.42E-08	6.72E+00	3.24E-08	3mm Sn	3.44	3.44E-08
3 mm Cu	0.95	4.90E-08	6.23E+00	4.78E-08	3.90E+00	3.12E-08	6.2mm W	3.29	3.50E-08
3 mm Sn	0.10	4.42E-08	1.49E+00	3.94E-08	1.87E+00	2.70E-08	1mm W 1.5mm Sn	2.76	3.18E-08
3 mm Sn	0.05	4.54E-08	1.22E+00	3.78E-08	1.32E+00	2.56E-08	3mm W 1mm Sn	1.29	3.02E-08
1 mm W 1.5 mm Sn	Too low	4.28E-08	1.01E-01	3.34E-08	9.66E-01	2.60E-08	10mm W	0.94	3.32E-08
1 mm W 1.5 mm Sn	Too low	4.14E-08	1.13E-01	3.14E-08	7.26E-01	2.62E-08	10mm W	0.75	3.38E-08

Table 3 Sample of FWHM of PITHON Shots

Note that PIN diode behind the heaviest filtering has a FWHM pulse width of about 42 ns while the PIN diode behind the lightest filtering has a FWHM pulse width of about 54 ns for shot number 7096 indicating that PITHON high energy (filtered) x-rays have the shorter pulse widths.

For higher energy operation, PITHON shot number 7148 (777-keV endpoint), similar results are tabulated in Table 3. The FWHM for heavy filtering (the high energy x-ray component) is 33 ns while light filtering results in a FWHM of 50 ns.

6 SUMMARY

This report documents in a summary fashion, experiments performed to validate that calculated photon spectra are reasonable for the PITHON flash x-ray machine when operated at endpoint energy ranging from 180 keV to 800 keV. This is the range of operation of the PITHON machine we used to obtain experimental data that have been and will be used for validating computer code models of Cable SGEMP, Box IEMP, and Connector IEMP phenomena.

While we found the calculated energy spectra to generally agree with our experimental LEDAS unfolded spectra, there were some differences. Code validation calculations can use both calculated and measured spectra at essentially the same PITHON endpoint energy for any individual experiment to determine, using computational simulation results, whether these spectral differences are significant. This information also helps to bound errors due to spectral uncertainties.

We found some variation in the time dependence of higher energy photons versus lower energy photons produced by the PITHON machine. Where these variations are important in calculating the experimental response, the temporal variations can be included in the computer models.

All experimental results are documented in an electronic data base that includes large tables summarizing all the results. We chose in this report to include pertinent experimental data and results, but not include the entire large data sets and all plots.

REFERENCES

1. J. L. Liscum-Powell, W.J. Bohnhoff, and C. D. Turner, "A Cable SGEMP Tutorial: Running CEPXS, CEPTRE and EMPHASIS/CABANA to Evaluate the Electrical Response of a Cable", SAND2007-2548, April 2007.

2. E. F. Hartman, T. A. Zarick, and T.J. Sheridan, "Validation Experiments for the RAMSES Cable SGEMP Analysis Codes", SAND2007-4463, August 2007.

3. E. F. Hartman, "Design Guide for Radiation Effects in Electronics", SAND2007-6124, September 2007.

4. J. C. Riordan and N. Qi, "Parametric Spectral Unfold for Differential Absorption Spectrometer", Final Report for Task Order No. 48, DTRA01-02-D-0005, Titan Pulse Sciences Division, San Leandro, CA, December 2004.

5. G. A. Carlson and L. J. Lorence, IEEE Transactions on Nuclear Science, Vol. 35, 1988.

6. J. C. Riordan, "PITHON High-Dose-Rate Reflex Triode Development, TSPD Final Report, November 2004, Titan Pulse Sciences Division.

7. W. H. Press et al, Numerical Recipes, pp 402-406, Cambridge Press (1992).

8. Private communication, Henry Moeller, SVIC (Boeing Co), Ogden, Utah.

DISTRIBUTION

1	MS 0311	J.M. Schare	02626
1	MS 0311	L.S. Weichman	02626
1	MS 0417	D.M. Fordham	00243
1	MS 0427	R A Paulsen, Jr.	02118
1	MS0429	R.C. Hartwig	02990
1	MS 0453	M.A. Rosenthal	02130
1	MS 0479	J.F. Gilbride	02138
1	MS 0481	J.F. Nagel Jr.	02137
1	MS 0523	L.A. Andrews	01733
1	MS 0523	J.E Christensen	01732
1	MS 0537	P.A. Molley	05351
1	MS 0574	B.C. Bedeaux	05924
1	MS 0970	A. J. Medina	05700
1	MS 1071	D.D. Chu	01730
1	MS 1106	K.A Mikkelson,	01342
1	MS11145	P.S. Raglin	01340
1	MS 1146	P.J. Griffin	01384
1	MS 1152	M. Kiefer	01652
1	MS 1152	C.D. Turner	01652
1	MS 1159	J.W. Bryson	01344
1	MS 1159	S.C. Jones	01344
1	MS 1159	V.J. Harper-Slaboszewicz	01344
1	MS 1159	C.A. Coverdale	01344
5	MS 1167	E.F. Hartman	01343
1	MS 1167	T.A. Zarick	01343
1	MS 1167	T.J. Sheridan	01343
1	MS 1167	E.L.Blansett	01343
1	MS 1167	S.D. Bonaparte	01343
1	MS 1167	K.M. Horn	01343
1	MS 1169	J.R. Lee	01300
1	MS 1179	W.C. Fan	01341
1	MS 1179	J. Powell	01341
1	MS 1179	M.A, Hedemann	01340
1	MS 1179	L.J. Lorence	01341
1	MS 1179	C.R. Drumm	01341
1	MS 1219	D.E. Beutler	05923
1	MS 9004	W.P. Ballard	08100
1	MS 9106	D.D Gehmlich	08226
1	MS 9154	E.B. Bochenski	08244
1	MS 9154	R.E. Oetken	08244.

1	MS 9018	Central Technical Files	08944
2	MS 0899	Technical Library	04536

1 Gary Lum
Lockheed Martin Missiles & Space
1111 Lockheed Way
Organization L4-01, Bldg 157
Sunnyvale, CA 94088

1 Thomas A. Stringer
ITT Advanced Engineering & Sciences
5009 Centennial Blvd.
Colorado Springs, CO 80919

3 John C. Riordan
L-3 Pulse Sciences
2700 Merced Street
San Leandro CA 94577

Sandia National Laboratories